Biointerface Research in Applied Chemistry

Original Research Article

Open Access Journal

Pt(II) complex @mesoporous silica: preparation, characterization and study of release

Maria Luisa Saladino [1,2,*], Simona Rubino [1], Paola Colomba [1], Maria Assunta Girasolo [1], Delia F. Chillura Martino [1,2], Caglar Demirbag [3], Eugenio Caponetti [1,2]

[1] Dipartimento Scienze e Tecnologie Biologiche, Chimiche e Farmaceutiche - STEBICEF and INSTM UdR - Palermo, Università di Palermo, Parco d'Orleans II, Viale delle Scienze pad.17, Palermo I-90128, Italy

[2] Centro Grandi Apparecchiature-ATeN Center, Università di Palermo, Via F. Marini 14, Palermo I-90128, Italy

[3] Marmara University, Faculty of Pharmacy, Department of Analytical Chemisty, Tibbiye Street 49, Haydarpasa 34668 Istanbul, Turkey

*corresponding author e-mail address: *marialuisa.saladino@unipa.it*

ABSTRACT

Cisplatin analogs, having cytotoxic activity higher than that exerted by cisplatin, have recently triggered considerable interest by the community. The cis-[PtCl$_2$(DMSO)HL]·2DMSO, where HL = 7-amino-2-(methylthio)[1,2,4]triazolo[1,5-a]pyrimidine-6-carboxylic acid, has shown a potent cytotoxic activity on HepG2 hepatocarcinoma cells, while under identical conditions, it did not affect normal immortalized human liver cells (Chang). In this work, the above complex has been incorporated into MCM41 mesoporous silica, pure and functionalized with amino group, which is considered one of the best host for a drug delivery system for carrying high dosages of a variety of drugs in their mesopores. Since the controlled release of an anticancer drug helps to maintain its therapeutic level for an extended time period while minimizing undesirable high peaks immediately following administration, the *in vitro* tests have been performed in order to obtain the corresponding drug release profile. The investigated system demonstrated to be an efficient system for pharmaceutic controlled release. A deepened characterization of the systems has been performed in order to known their structure and features and to speculate the mechanisms involved in the release.

Keywords: *MCM41, amino groups, Cisplatin analogs, XRD, ^{29}Si {^1H} CP-MAS NMR, controlled release.*

1. INTRODUCTION

Drug carriers play a critical role for the loading and the release of the drug. Promising frontiers is represented by a new class of innovative medicines based on directional transport vehicles "drug delivery" and consist of assembled structures carrier (nano)-drug.

Silica-based materials, nontoxic, biocompatible, have been used as adjuvant and excipient in pharmaceutical technology. Within this class of compounds, mesoporous silica materials such as MCM41, SBA-15 and HMS have been investigated for medication and drug delivery due to their properties. The large surface area and pore volume, together with the nanoporous structure facilitate the control release of drugs. Many papers report the incorporation and the release of drugs and vitamins from MCM41 framework [1-5]. The resulting materials exhibit unique physicochemical properties determined by the state of the guest molecules, in addition to the nature of the mesoporous and its features (structure and pore size) and to the functional groups on the surface [6,7]. In fact, the functionalization with several kinds of molecules of the porous internal surface can influence the physical - chemical interactions between the mesoporous and the drug, thus controlling the delivery in terms of kinetics. In particular, the synthetic drug delivery systems have great potential to overcome the problems associated with systemic toxicity of chemotherapy, including treatment with platinum-based drugs [8]. For these reasons, some authors have reported the incorporation of the cisplatin in mesoporous compounds investigating the controlled release *in vitro* at human condition [9-14]. In the meantime, the discovery of successful candidates and strategies

for the selective directionality of platinum drugs is a very active area of research. Novel platinum(II) complexes including nanotechnology applications and complexes containing heterocyclic ligands with N and S donor atoms are under study with the aim to reduce and overcome the toxicity of cisplatin and its analogues, and to decrease the nephrotoxicity of platinum complexes [15].

Recently, a new anticancer drug, the cis-[PtCl2(DMSO)HL]·2DMSO, where HL = 7-amino-2-(methylthio)[1,2,4]triazolo[1,5-a]pyrimidine-6-carboxylic acid, hereafter called complex (1), has been synthesized and tested by some of us [15]. The class of compounds of triazolopyrimidine shows antimicrobial and antitumor properties and can be used to study metal-ligand interaction in biological systems. The complex (1) exhibited a very marked biological activity on HepG2 hepatocarcinoma cells while under identical conditions it did not affect normal immortalized human liver cells (Chang Liver cells). The mechanism of anti-proliferative effect of the complex (1) on HepG2 was pro-apoptotic and the antiproliferative efficacy was twofold higher than that shown by cisplatin.

In this work, due to the observed properties and the potential in the enhanced anticancer activity, the complex (1) has been incorporated in a mesoporous materials in order to obtain a controlled release system. Similar study on cisplatin analogues has not yet investigated to the best of our knowledge. Since many authors claim the importance of a proper support selection as a strategy to control the delivery of active molecules, making a correlation between textural properties and release kinetics, the

mesoporous silica MCM41 and the mesoporous silica MCM41 functionalized with amino groups (MCM41-NH$_2$) have been used as host for this study. The role of the amino group in the encapsulation efficiency and in the release kinetics of the complex (1) has been thus investigated.

The characterization of the materials was performed by using X-ray Diffraction (XRD), Gas adsorption, ^{29}Si Cross Polarization - Magic Angle Spinning NMR Spectroscopy (^{29}Si {^{1}H} CP MAS NMR). The loading capacity and the release of complex (1) in a phosphate buffer solution (PBS) at pH 7.4 and 37°C in order to simulate the human conditions was evaluated by using the Uv-vis Spectroscopy.

2. EXPERIMENTAL SECTION

2.1. **Materials.** Tetraethoxysilane (TEOS, 99%, Fluka), cetyltrimetylammonium bromide (CTAB, 98%, Aldrich), ammonia solution (28%, Aldrich), ethanol (99.8%, Fluka), 3-aminopropyl triethoxysilane (APTES 98%, Aldrich), anhydrous toluene (99.8%, Aldrich), diethyl ether (99.9%, Aldrich), dichloromethane (99.5%, Aldrich), chloroform (99.5%, Aldrich), phosphate buffer solution (PBS, 0.1M, pH=7.5, Aldrich), were used as received. Solutions were prepared by weight adding conductivity grade water.

2.2. **Samples preparation.** The syntheses of the complex (1) and of the MCM41 mesoporous silica are reported elsewhere [15,16]. The MCM41-NH$_2$ was prepared as follows. MCM41 silica was dehydrate at 60°C for 2 h to remove physisorbed water. 1 g of MCM41 was thus dispersed in 40 mL of anhydrous toluene and 1.2 mL of APTES, used as functionalizing agent, was added to the dispersion. The reaction was carried out at room temperature for 20 h and then refluxed for 4 h. The suspension was filtered and washed with a 1:1 mixture of diethyl ether and dichloromethane and dried at 60°C for 3 days.

The complex (1) loading was performed by following the experimental procedure reported by Mori [14]: MCM41 and MCM41-NH$_2$ samples were soaked, under continuous magnetic stirring for 24 h at room temperature, into a chloroform solution of complex (1) (0.06 mg/mL). The complex (1) to the mesoporous weight ratio was 1:4. The loaded samples were recovered by vacuum filtration, washed with chloroform and dried under vacuum overnight. The supernatant was collected and analysed using UV-vis spectroscopy to determine the unloaded amount of complex (1) and by difference the loaded quantity on the mesoporous.

2.3. **Instrumentation.** UV–vis absorption spectra of solutions of complex (1) were recorded in the range 200–400 nm using a double beam Beckman DU-800 spectrophotometer with a resolution of 1.0 nm. In order to eliminate the effect of instrumental errors and of particle diffusion, the value of absorbance at 400 nm was subtracted to each spectrum.

X-ray Diffraction (XRD) patterns were acquired by using a PW 1050 Philips diffractometer in the Bragg-Brentano geometry equipped with a Cu Coolidge tube and a scintillation detector beam (40 kV, 30 mA, step 0.05° , counting time 5s/step). The instrument resolution (divergent and antiscatter slits of 0.5°) was determined using standards free from the effect of reduced crystallite size and lattice defects.

N$_2$ absorption-desorption isotherms were registered at 77 K using a Quantachrome Nova 2200 Multi-Station High Speed Gas Sorption Analyser. Samples were outgassed for 3 hr at room temperature in the degas station. Adsorbed nitrogen volumes were normalized to the standard temperature and pressure.

^{29}Si {^{1}H} CP–MAS NMR spectra were obtained at room temperature on a Bruker Avance II 400 MHz (9.4 T) spectrometer operating at 79.4 MHz. Samples were compressed in 4 mm zirconia rotors with Kel-F (PCTFE) caps. The ^{29}Si spectra were acquired using a MAS rate of 5 kHz, 4096 scans, contact time of 8 ms, an excitation pulse on the ^{1}H nucleus of 4.15 μs and repetition delay of 8 s. The contact time values were optimized on the samples through variable contact time (VCT) experiments and the optimization of the Hartmann–Hahn condition [17] was obtained by means of a Q8M8 (Si[(CH$_3$)$_3$]$_8$Si$_8$O$_{20}$) standard.

2.4. **Study of complex (1) release.** *In vitro* drug release was evaluated at 37±1 °C in 0.1 M phosphate buffer solution (PBS) having pH 7.4 to simulate the physiological pH of blood. 40 mg of complex (1) loaded samples were placed with 2 mL of PBS in a closed 3,5 kDa dialysis membrane tube (Spectra/Por 3 Dialysis membrane. 3,5 MWCO, 11,5 mm diameter), and then in a Nalgene-flask filled with PBS. The total amount of PBS was 20 mL. The flask was closed and kept under shaking (60 rpm) at 37±1 °C. At scheduled time intervals, an aliquot of the solution was taken and the UV-Vis spectrum was recorded.

3. RESULTS SECTION

3.1. Determination of the complex (1) amount loaded on the mesoporous materials. For calibration purposes, five standard solutions of complex (1) were prepared in chloroform in the range of 0.01-0.08 mg/mL. The UV-vis spectra of the standard solutions are reported in Figure S1 of the Support Information (S.I.). The calibration curve, obtained by plotting the absorbance values of the band maximum (λ_{max} = 300 nm) versus the standard solution concentrations, is reported in Figure S2 of the S.I..

The complex (1) encapsulation efficiency % (EE%) of MCM41 and MCM41-NH$_2$ samples were evaluated using the following method: the filtrate was collected and analysed using UV-vis spectroscopy.

From the absorbance values of the band maximum, the amount of unloaded complex (1) was derived. The loaded complex (1) amount was calculated as difference between the stoichiometric quantity and the complex (1) unloaded.

The EE% was 75.0 $_{w/w}$ % and 83.3 $_{w/w}$ % for the MCM41 and the MCM41-NH$_2$ samples, respectively (all loading measurements were performed in triplicate). The higher value obtained for the functionalized system is an indication that some specific interactions between the amino group and the complex (1) may be established.

On the other hand, the obtained high value for the MCM41 is an indication that electrostatic and dipolar interactions, favored by the solvent, may have a role in the loading, thus suggesting that functionalization is not the major factor boosting drug uptake.

3.2. Structural investigation. The XRD patterns of MCM41 and of MCM41-NH$_2$ samples are reported in Figure 1.
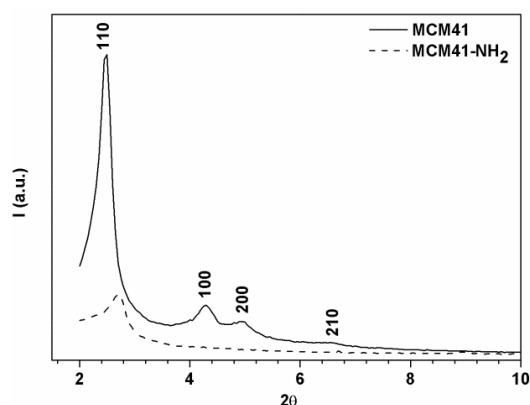

Figure 1. XRD patterns of MCM41 and of MCM41-NH$_2$ samples.

The XRD pattern of MCM41 is characteristic of the hexagonal structure: a peak of high-intensity (100) and three reflections of low-intensity (110, 200 and 210) [16,18,19]. No reflection was observed in the high angle region of XRD patterns for both samples.

The mesoporous structure is basically preserved after the functionalization (MCM41-NH$_2$ sample) even if, comparing the two XRD patterns, a shift and a decrease of the (100) peak together with the disappearing of the secondary peaks is observed. The adjacent pores centre-centre distance, a_0, of all samples was calculated by means of the equation $\alpha_0 = \frac{2d_{100}}{\sqrt{3}}$ [20], where d$_{100}$ is the d$_{100}$ spacing computed by using the Bragg's law. For each sample, the calculated a$_0$ values are reported in the Table 1.

Table 1. Structural data of samples (a$_0$, lattice parameter; S$_{BET}$, specific surface area; w$_{BJH}$, pore width; Vt, total pore volume).

Sample	α_0 (Å)	S$_{BET}$ (m^{2}g^{-1})*	w$_{BJH}$ (Å)	V$_t$ (cc/g)
MCM41	41(1)	1276	35	1.35
MCM41/complex (1)	39(1)	393	33	0.47
MCM41-NH$_2$	38(1)	87	37	0.07
MCM41-NH$_2$/complex (1)	38(1)	23	37	0.02

* The uncertainty on the S$_{BET}$ values is 5%.

The decrease of α_0 as a consequence of the functionalisation can be ascribed to the formation of hydrogens bonds among the amino groups that promote a shrinking of the porous structure [13]. The XRD patterns of the complex (1) loaded samples are reported in Figure 2.

For comparison the XRD pattern of MCM41 and of MCM41-NH$_2$ samples are reported in the same figures. In general,

the XRD patterns showed, for both loaded samples, that the hexagonal lattice symmetry is maintained after the loading indicating that the porous structure of the MCM41 is maintained as a consequence of the loading.

The XRD patterns of the loaded samples show a decrease in intensity of the (100) peak respect to that of the unloaded one as a consequence of a variation in the electron density. For both loaded samples, the α_0 value is 39(1) Å. It does not significantly change with respect to the unloaded samples. Detailed analysis of these small changes is outside the scope of this work. Similar results are reported in literature [21] where several factor such interactions between molecules and changes in overall background scattering of X-rays are taken into account.
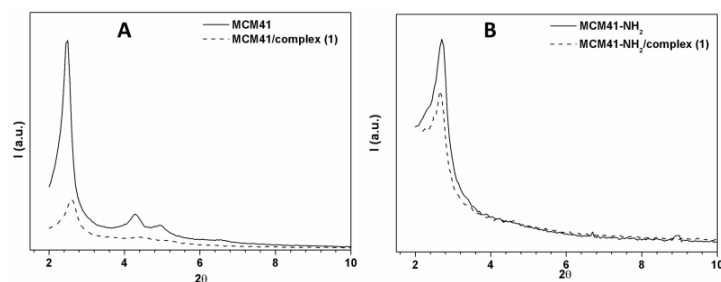

Figure 2. XRD patterns of A) MCM41 and of MCM41/complex (1) and of B) MCM41-NH$_2$ and of MCM41-NH$_2$ /complex (1) samples.

Since the pore diameter is 41 (1) and 38 (1) Å respectively for MCM41 and for MCM41-NH$_2$ and the size of complex (1) molecule is ca. 9 Å, diffusion of the drug is unlikely to be the limiting factor for complex (1) uptake. Hence, the differences found in the amount of drug loaded are likely to reflect corresponding differences of interaction energy between the drug molecule and the pore wall, which are expected to depend on the functional group.

Nitrogen adsorption-desorption isotherms were registered to obtain information about the specific surface area (S$_{BET}$) and the total pore volume (V$_t$). Some of them are reported in Figure S3 of the S.I.. According to IUPAC [22] the characteristic type IV-isotherms is obtained for the MCM41.

Once functionalized, the obtained isotherm of the MCM41-NH$_2$ is of type I. Similar results have been reported by Zeng at al [23] who hypothesize the presence of secondary interparticle mesopores, which are favorable for drug delivery applications. The same type of isotherm has been obtained as a consequence of the complex(1) uptake for both MCM41 and MCM41-NH$_2$.

The S$_{BET}$ was calculated by using the BET method [24] in the relative adsorption pressure (P/P$_0$) range from 0.045 to 0.250. The V$_t$ was obtained from the nitrogen amount adsorbed in correspondence of P/P$_0$ equal to 0.99.

S$_{BET,}$ and V$_t$, are reported in Table I. As expected, after the functionalisation the surface area and the pore volume of MCM41 significantly decrease as well as after the loading. It is well known that the aminopropyl functional groups added with the used post-synthesis procedure tend to distribute near the entrance of the mesoporous channels, thus explaining the observed high decrease of surface area [25].

The findings also evidence the presence of the drug within the pores. During the loading the chloroform solution containing the complex (1) diffuse into the pores. After the chloroform

removal and the drying process the molecules remain trapped partially obstructing the mesochannels, analogously to the ones reported by Zeng at al [25].

The ^{29}Si $\{^1H\}$ CP-MAS NMR spectra of MCM41, MCM41/complex (1), MCM41-NH$_2$, MCM41-NH$_2$/complex (1) samples are reported in Figure 3.
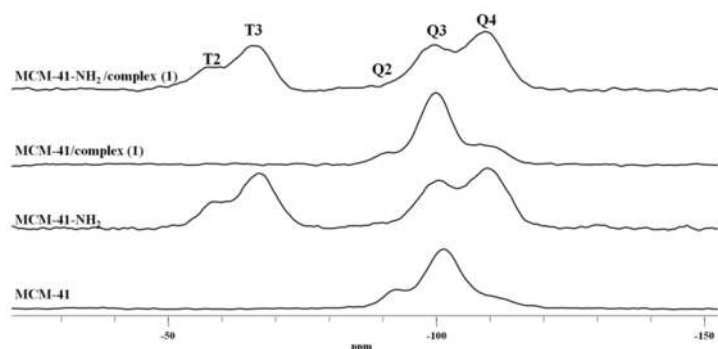

Figure 3. ^{29}Si $\{^1H\}$ CP-MAS NMR spectra of MCM41, MCM41-NH$_2$, MCM41/complex (1), and MCM41-NH$_2$/complex (1) samples.

The ^{29}Si $\{^1H\}$ CP-MAS NMR spectrum of MCM41 shows three broad, Q^2, centred at around -90 ppm, due to the geminal silanols, , Q^3, at around -100 ppm, due to the silicon atoms bearing one hydroxyl group and, Q^4, at around -109 ppm, due to the silicon atoms without hydroxyl groups [16,18,19].

In the ^{29}Si $\{^1H\}$ CP-MAS NMR spectrum of MCM41-NH$_2$ two new resonances (T^2 and T^3) corresponding to two different environments for the siloxane groups in the functionalized material are present [20]. The T^3 at -66.7 ppm and the T^2 at -58.7 ppm are due to RSi(OSi)$_3$ terminal units and to (SiO)$_2$R-Si(OH) cross-linked units, respectively. The presence of T^2 and T^3 peaks evidences the covalent linkage between the aminopropyl groups and the silica surface. In addition, as the grafting reaction takes place, a marked increase of the Q^4 peak intensity together with a decrease of the Q^2 peak is observed. This indicates the conversion of the (SiO)$_3$Si–OH species to fully condensed species occurred due to the grafting.

Knowing that the samples show the same chemical shifts and the same cross polarization dynamic, and that the variation of the contact time does not modify the relative intensity distribution of the signals, the deconvolution of each spectrum has been performed to calculate the single contributions of the signal, as performed by some of us [16] for the quantification of the different silicon groups. The obtained values are reported in Table 2. As reported by some authors, the relative integrated intensities of NMR signals of the organosiloxane ($\sum$Tm) and siloxane ($\sum$Qm) (T/Q ratio) can be employed to estimate the incorporation degree of functional groups [25]. The T/Q ratio for the MCM41-NH$_2$ is 0.63, implying high surface coverage of amino groups, which were available for incorporation processes of drug molecules. For the MCM41-NH$_2$/complex(1) this value is 0.57, roughly coincident with the previous one in the limit of the experimental errors. This means that the silicon environment unchanged in the presence of the complex (1). However, looking for the area of single contributes, for the MCM41-NH$_2$ /complex(1) sample, Q2 increase of 91%, Q3 decrease of 4% and Q4 increase of 0.6%, T2

increase of 68% and T3 decrease of 25%, respect to the values calculated for the MCM41-NH$_2$.

Notwithstanding, the opposite trend observed for the MCM41/complex(1), where Q2 decrease of 30%, Q3 increase of 5% and Q4 increase of 2.7%, all these findings indicate that the complex (1) influence the dynamic of cross polarization and it is an indication that the drug is located inside the pore of the two mesoporous.

Table 2. Peaks areas obtained by deconvolution of the ^{29}Si $\{^1H\}$ CP-MAS NMR area.

	10^6 T2	10^6 T3	10^6 Q2	10^6 Q3	10^6 Q4	T/Q ratio
MCM41	-	-	214.5	1057	332.1	-
MCM41/complex (1)	-	-	154.3	1131	347.3	-
MCM41-NH$_2$	178.8	487.	24.1	452.2	574.9	0.63
MCM41-NH$_2$/complex(1)	378.6	460.7	64.0	604.4	797.1	0.57

3.3. Study of the release. The drug release profile is of great importance in applying the synthesized systems to a practical drug delivery for cancer chemotherapy. For calibration purposes, five standard solutions of complex (1) in PBS were prepared in the range of 0.0025-0.015 mg/mL. The UV-vis spectra of the standard solutions are reported in Figure S5 of the S.I.. The calibration curve, obtained by plotting the absorbance values of the band maximum (λ_{max} = 246 nm) versus the standard solution concentrations, is reported in Figure S6 of the S.I.

In order to evaluate the amount of the complex (1) released in the PBS solution, the Uv-vis spectra were acquired at scheduled time intervals. The UV-vis spectrum of each aliquot taken by the MCM41-NH$_2$/complex (1) and the MCM41/complex (1) systems is reported in Figure S7 and S8, respectively.

The amount of released complex (1) was calculated by the maximum of the absorption band at 246 nm on the basis of the calibration curve. The release profile of the complex (1) from both loaded functionalized and non-functionalized samples was studied as a function of time and the results are reported in Figure 4.
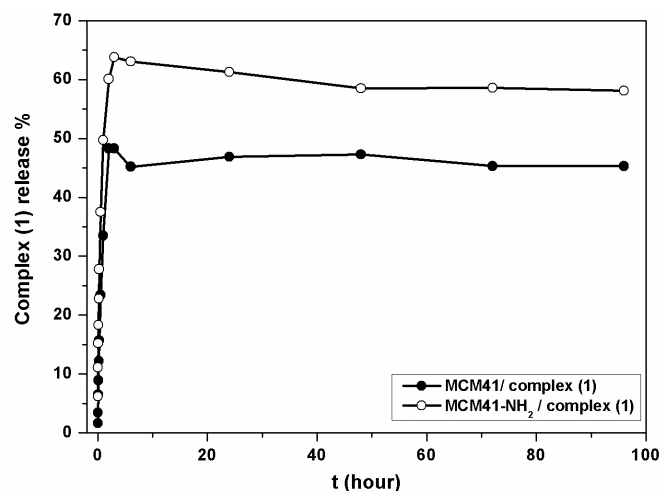

Figure 4. Release profile of complex (1) in PBS solution from the MCM41/complex (1) and MCM41-NH$_2$/complex (1) samples.

As can be seen, the two systems exhibit different drug release profiles. In this sense, some aspects are worth to be considered. The *in vitro* release of complex (1) from MCM41 and MCM41-NH$_2$ mesoporous has been performed for 96 hours. After 2 hours the MCM41/complex (1) system reached maximum release ratio, while the MCM41-NH$_2$/complex (1) release in 3 hours. The maximum released complex (1) ratios are 48.3 % and 63.8 % for pure and amino functionalized MCM41 loaded samples, respectively. MCM41 system reached the plateau concentration faster than MCM41-NH$_2$ system. The functionalized MCM41 shows slow complex (1) release. Many authors explain the different release taking in account the interactions between the drug and the functional groups of the mesoporous. In this case, the different release rate may be due to the properties of the modified MCM-41. Respect to the MCM41, in the MCM41-NH2 the presence of the hydrocarbon chains confer the pore surface a rather hydrophobic character, hence a higher affinity for molecules of lower polarity, but at the same time the amino groups could interact by means of an hydrogen bonding interactions with the nitrogens of the amino groups or with the oxygens of the carboxylic groups of the complex (1). These interaction are responsible of the higher loading, having as medium the chloroform, in the mesoporous functionalised with amino groups.

4. CONCLUSIONS

This work reports a promising suitably strategy for the controlled release of drugs like the cisplatin derivatives in therapeutic applications. The preparation and the characterization of two drug delivery systems, MCM41/complex (1) and MCM41-NH$_2$/complex (1), was reported. In both case, the maintenance of the hexagonal structure after the functionalization and the complex (1) loading was checked by XRD. Experimental results showed that ordered mesoporous structure is preserved after the functionalization and that the complex (1) does not affect the hexagonal structures. The surface area and the pore volume of the mesoporous decrease with the complex (1) loading indicating that the molecule is inside the pores. NMR investigation show that the different silicon environments are influenced by the drug in terms of magnetisation transfer, confirming that the drug is inside the pores.

MCM41-NH$_2$ showed a greater drug uptake than pure MCM41 and, in addition, it is more effective than pure MCM41 as a carrier of controlled delivery of complex (1) releasing more than 63 % of complex (1) at first 24 hours. Probably, it is due to hydrogen bonding interaction between the amino groups on silica walls and some groups of complex (1). These studies clearly shows that the complex (1) can be efficiently released from the amino-functionalized MCM41 mesoporous silica. The mesoporous materials have many advantages as drug delivery systems but there are many questions about their behaviors *in vivo* conditions such as pharmacokinetics, pharmacodynamics and toxicity etc.

Supporting Information Available. UV spectra, Nitrogen adsorption-desorption isotherms and relative calibration curves.

5. REFERENCES

[1] Xue J. M., Shi M., PLGA/Mesoporous hybride structure for controlled drug release, *J. of Controlled Release,* 98, 209–217, **2004**.

[2] Wu Z., Jiang Y., Kim T., Lee K., Effects of surface coated on the controlled release of vitamin B1 from mesoporous silica tablets, *J. of Controlled Release*. 119, 215–221, **2007**.

[3] Izquierdo-Barb I., Sousa E., Doadrio J. C., Doadrio A. L., Perez Pariente J., Martınez A., Babonneau F., Vallet-Regı M., Influence of mesoporous structure type on the controlled delivery of drugs: release of ibubrofen from MCM-48, SBA-15 and functionalized SBA-15, *J. Sol-Gel Sci Technol*, 50, 421–429, **2009**.

[4] Manzano M., Aina V., Arean C.O., Balas F., Cauda V., Colilla M., Delgado M. R., Vallet-Regi M., Studies on MCM-41 mesoporous silica for drug delivery: effect of the particle morphology and amine functionalization, *Chem. Engineering* J., 137, 30–37. **2008**.

[5] Chen X., Cheng X., Soeriyadi A.H., Sharon M., Xun S., Scott Jason A., Lowe Stuart B., Kavallaris M., Gooding Justin J., Stimuli-responsive functionalized mesoporous silica nanoparticles for drug release in response to various biological stimuli, *Biomaterials Science*, 2, 121-130, **2014**.

[6] Pérez-Esteve E, Ruiz-Rico M., de la Torre C., Villaescusa L.A., Sancenón F., Marcos Pedro Amorós M.D., Martínez-Máñez R., Manuel Barat, *J. Food Chemistry*, 196, 66–75, **2016**.

[7] Ayad M.M., Salahuddin N.A., Abu El-Nasr A., Torad N.L., Microporous and Mesoporous Materials, 229, 166-177, **2016.**

[8] Haxton K.J., Burt H.M., Polymeric drug delivery of platinum-based anticancer agents, *J. Pharm Sciences*, 98, 2299-2316, **2009**.

[9] Gu J., Liu J., Li Y., Zhao W., Shi J., One-spot synthesized of mesoporous silica nanocarriers with tunable particle sizes and pendent carboxylic groups for cisplatin delivery *Langmuir*, 29, 403−410, **2013**.

[10] Gu J., Su S., Li Y., He Q., Zhong J., Shi J., Surface modification-complexation strategy for cisplatin loading in mesoporous nanoparticles, *J. Phys. Chem. Lett.*, 1, 3446–3450, **2010**.

[11] Mukhopadhyay K., Bibhas R.S., Chaudhari R.V. Anchored, Pd complex in MCM-41 and MCM-48: novel heterogenous catalysts of hydrocarboxylation of aryl olefins and alcohols, *J. Am. Chem. Soc.,* 124, 9692-9693, **2002**.

[12] Tao Z., Xie Y., Goodisman J., Asefa T., Isomer-dependent absorption and realese of cis- and trans-platin anticancer drugs by mesoporous silica nanoparticles, *Langmuir*, 26(11) 8914–8924, **2010**.

[13] Arean C.O., Vesga M.J., Parra J.B., Delgado M.R., Effects of amine and carboxylic functionalization of sub-micrometric MCM-41 spheres on controlled release of cisplatin, *Ceramics International*, 39, 7407–7414, **2013**.

[14] Mori K., Watanabe K., Kawashima M., Che M., Yamashita H., Anchoring of Pt[II] pyridyl complex to mesoporous silica materials: enhanced photoluminescence emission at room temperature and photoxidation activity using molecolar oxygen, *J. Phys. Chem., C* 115, 1044–1050, **2011**.

[15] Rubino S., Di Stefano V., Attanzio A., Tesoriere L., Girasolo M.A., Nicolò F., Bruno G., Synthesis, spectroscopic characterization and antiproliferative activity of two platinum complexes containing N-donar heterocycles, *Inorganica Chimica Acta,* 418, 112-118, **2014**.

[16] Saladino M.L., Kraleva E., Todorova S., Spinella A., Nasillo G., Caponetti E., Synthesis and characterization of mesoporous Mn-MCM-41 materials, *J. of Alloys and Compounds*, 509, 8798– 8803, **2011**.

[17] Hartmann S.R., Hahn E.L., Nuclear double resonance in the rotating frame., *Phys. Rev.,* 128, 2042, **1962**.

[18] Aguado J., Serrano D.P., Escola J.M., A sol-gel approach for the room temperature synthesis of Al-containing micelle-templated silica, *Microporous Mesoporous Mater.*, 34, 43, **2000**.

Maria Luisa Saladino, Simona Rubino, Paola Colomba, Maria Assunta Girasolo, Delia F. Chillura Martino, Caglar Demirbag, Eugenio Caponetti

[19] Manzano M., Aina V., Areán C.O., Balas F., Cauda V., Colilla M., Delgado M.R., Vallet-Regí M., Studies on MCM-41 mesoporous silica for drug delivery: effect of particle morphology and amine functionalization, *Chemical Engineering Journal*, 137, 30–37, **2008**.

[20] La Parola V., Longo A., Venezia A.M., Spinella A., Caponetti E., Interaction of Gold with Co-Condensed and Grafted HMS-SH Silica: a 29Si {1H} CP-MAS NMR Spectroscopy, XRD, XPS and Au LIII EXAFS, Study *Eur. J. Inorg. Chem.*, 3628–3635, **2010**.

[21] He Q., Shi J., Mesoporous silica nanoparticle based nano drug delivery systems: synthesis, controlled drug release and delivery, pharmacokinetics and biocompatibility, *J. Mater. Chem.*, 21, 5845–5855, **2011**.

[22] Gregg S.J., Sing K.S.W., Adsorption, Surface Area and Porosity, 2nd edition, Academic Press, London, **1982**.

[23] Zeng W., Qian X.-F ., Zhang Y-B., Yin J., Zhu Z.Z. *Materials Research Bulletin,* 40, 766–772, **2005**.

[24] Brunauer S., Emmett P.H., Teller E., *J. Am. Chem. Soc.*, 60, 309, **1938**.

[25] Yang C.-M., Liu P.-H., Ho Y.-F., Chiu C.-Y., Chao K.-J., *Chem. Mater.,* 15, 275–280, **2003**.

6. ACKNOWLEDGEMENTS